D10488

ADVMEW
ISSN 0935-9648
Vol. 18, No. 21
November 3, 2006

WILEY-VCH

ADVANCED MATERIALS

Buckled Ribbons of GaAs for Flexible Electronics

DOI: 10.1002/adma.200600646

Buckled and Wavy Ribbons of GaAs for High-Performance Electronics on Elastomeric Substrates**

By *Yugang Sun*, *Vipan Kumar*, *Ilesanmi Adesida*, and *John A. Rogers**

Performance capabilities in traditional microelectronics are measured mainly in terms of speed, power efficiency, and level of integration. Progress in other, more recent, forms of electronics is driven instead by the ability to achieve integration on unconventional substrates (e.g., low-cost plastics, foils, paper) or to cover large areas.[1,2] For example, new forms of X-ray medical diagnosis might be achieved with large-area imagers that can conformally wrap around the body and digitally image the desired tissue.[3] Lightweight, wall-size displays or sensors that can be deployed onto a variety of surfaces and surface shapes might provide new technologies for architectural design. Various materials including small organic molecules,[4–8] polymers,[9] amorphous silicon,[10–12] polycrystalline silicon,[13–16] single crystalline silicon nanowires,[17,18] and microstructured ribbons[19–22] have been explored to serve as semiconductor channels for the type of thin-film electronics that might support these and other applications. These materials enable transistors with mobilities that span a wide range (from 10^{-5} to 500 $cm^2 V^{-1} s^{-1}$), and in mechanically bendable thin-film formats on flexible substrates. Applications with demanding high-speed operations, such as large-aperture interferometric synthetic aperture radar (InSAR) and radio frequency (RF) surveillance systems, require semiconductors with much higher mobilities, such as GaAs or InP. The fragility of single crystalline compound semiconductors creates a number of fabrication challenges that must be overcome in order to fabricate high-speed, flexible transistors with them. We recently established a practical approach to build metal semiconductor field-effect transistors (MESFETs) on plastic substrates by using printed GaAs wire arrays created from high-quality bulk wafers.[23,24] These devices exhibit excellent mechanical flexibility and unity current gain frequencies (f_T) that approach 2 GHz, even in moderately scaled devices (e.g., micrometer gate lengths). The work described in this article demonstrates GaAs ribbon based MESFETs (as opposed to our previously reported wire devices) designed with special geometries that provide not only bendability, but mechanical stretchability to levels of strain (strain ranges of > 20 %) that significantly exceed the intrinsic yield points of GaAs itself (ca. 2 %). The resulting type of stretchable, high-performance electronic systems can provide extremely high levels of bendability and the capacity to integrate conformally with curvilinear surfaces. The work that we report on this GaAs system extends our recently described "wavy" silicon[25] in four important ways: i) it demonstrates stretchability in GaAs, a material that is in practical terms much more mechanically fragile than Si; ii) it introduces a new "buckled" geometry that can be used for stretchability together with or independently of the previously described "wavy" configuration; iii) it achieves a new class of stretchable devices (MESFETs); and iv) it demonstrates stretching over a larger range and with greater symmetry in compression/tension than that previously achieved in silicon.

Figure 1 illustrates steps for fabricating stretchable GaAs ribbons on an elastomeric substrate made of poly(dimethylsiloxane) (PDMS). The ribbons were generated from a high-quality bulk wafer of GaAs with multiple epitaxial layers. The wafer was prepared by growing a 200 nm thick AlAs layer on a (100) semi-insulating GaAs (SI-GaAs) wafer, followed by sequential deposition of a SI-GaAs layer with a thickness of 150 nm and Si-doped n-type GaAs layer with a thickness of 120 nm and a carrier concentration of 4×10^{17} cm^{-3}. A pattern of photoresist lines defined parallel to the $(0\bar{1}\bar{1})$ crystalline orientation served as masks for chemical etching of the epilayers (including both GaAs and AlAs). Anisotropic etching with an aqueous etchant of H_3PO_4 and H_2O_2 isolated these top layers into individual bars with lengths and orientations defined by the photoresist[26,27] and with side walls that form acute angles relative to the wafer surface. Removing the photoresist after the anisotropic etching and then soaking the wafer in an ethanol solution of HF (2:1 in volume between ethanol and 49 % aqueous HF) removed the AlAs layer and released ribbons of GaAs (n-GaAs/SI-GaAs). The use of ethanol instead of water for this step reduced cracking that can occur in the fragile ribbons resulting from the action of capil-

[*] Prof. J. A. Rogers, Dr. Y. Sun[+]
Department of Materials Science and Engineering
Beckman Institute and Frederick Seitz Materials Research Laboratory
University of Illinois at Urbana-Champaign
Urbana, IL 61801 (USA)
E-mail: jrogers@uiuc.edu
Dr. V. Kumar, Prof. I. Adesida
Department of Electrical and Computer Engineering
Micro and Nanotechnology Laboratory
University of Illinois at Urbana-Champaign
Urbana, IL 61801 (USA)
[+] Present address: Center for Nanoscale Materials, Argonne National Laboratory, Argonne, IL 60439, USA.

[**] This work was supported by the U.S. Department of Energy under grant DEFG02-91-ER45439. The fabrication and measurements were carried out using the facilities located in the Microfabrication Laboratory and Center for Microanalysis of Materials of Frederick Seitz Materials Research Laboratory, which are supported by Department of Energy. The authors thank Dr. Zheng-Tao Zhu for help in AFM measurement and Mr. Matthew A. Meitl for useful discussion.

ADVANCED MATERIALS

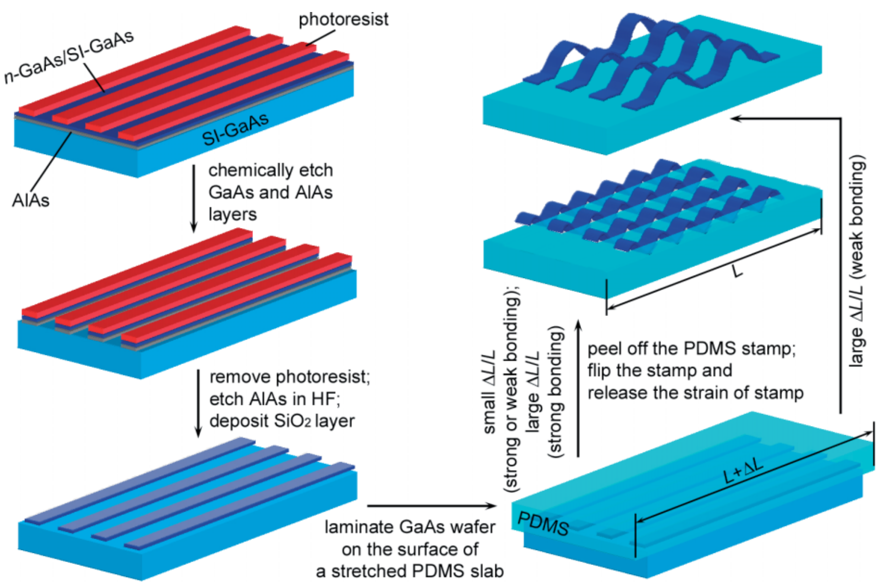

Figure 1. Schematic illustration of steps for generating "buckled" and "wavy" GaAs ribbons on PDMS substrates. The left bottom frame shows the deposition of thin SiO_2 on the surfaces of the ribbons to promote strong bonding to the PDMS. This bonding leads to the formation of the wavy geometry shown in the right middle frame. Weak, van der Waals bonding (and moderate to high levels of prestrain) leads to the buckled geometry, as shown in the right top frame.

strong bonding interaction between the ribbons and the substrate. A different type of geometry, consisting of aperiodic "buckles" with relatively large amplitudes and widths, formed in the case of weak interaction strengths and large prestrains (right, top frame). In addition, our results show that both kinds of structures — buckles and waves — can coexist in a single ribbon whose flexural rigidity varies along its length (for example, because of thickness variations associated with device structures).

Figure 2 shows several microscopy images of wavy GaAs ribbons with thicknesses of 270 nm (including both n-GaAs and SI-GaAs layers) and widths of 100 µm (all of the ribbons discussed in this paper have widths of 100 µm) formed with strong bonding between PDMS (thickness of ca. 5 mm) and ribbons. The fabrication followed the procedures for strong bonding, using 2 nm Ti and 28 nm SiO_2 layers on

lary forces during drying. The lower surface tension of ethanol compared with water also minimized drying induced disorder in the spatial layout of the GaAs ribbons. In the next step, the wafer with released GaAs ribbons was contacted to the surface of a prestretched flat slab of PDMS, with the ribbons aligned with the stretching direction. In this case, van der Waals forces dominate the interaction between PDMS and GaAs. For cases that require stronger interaction strength, we deposited a thin layer of SiO_2 onto the GaAs, and exposed the PDMS to ultraviolet induced ozone (i.e., product of oxygen in air) immediately prior to contact. The ozone creates –Si–OH groups on the surface of PDMS that react with the surface of the SiO_2 upon contact to form bridging siloxane –Si–O–Si– bonds. (The deposited SiO_2 is discontinuous at the edges of each ribbon because of the geometry of their sidewalls.)[27] For both the weak and strong bonding procedures, peeling the PDMS from the mother wafer transferred all the ribbons to the surface of the PDMS. Relaxing the prestrain in the PDMS led to the spontaneous formation of large-scale buckles and/or sinusoidal wavy structures along the ribbons. The geometry of the ribbons depends strongly on the prestrain (defined by $\Delta L/L$, see Fig. 1) applied to the stamp, the interaction between the PDMS and the ribbons, and the flexural rigidity of the ribbons. For the ribbons investigated here, small prestrains (<2 %) created highly sinusoidal "waves" with relatively small wavelengths and amplitudes (right, middle frame), for both the strong and weak interaction cases. These geometries in GaAs are similar to those that we recently reported for Si.[25] Higher prestrains up to ca. 15 % can be applied to create similar type of waves where there is a

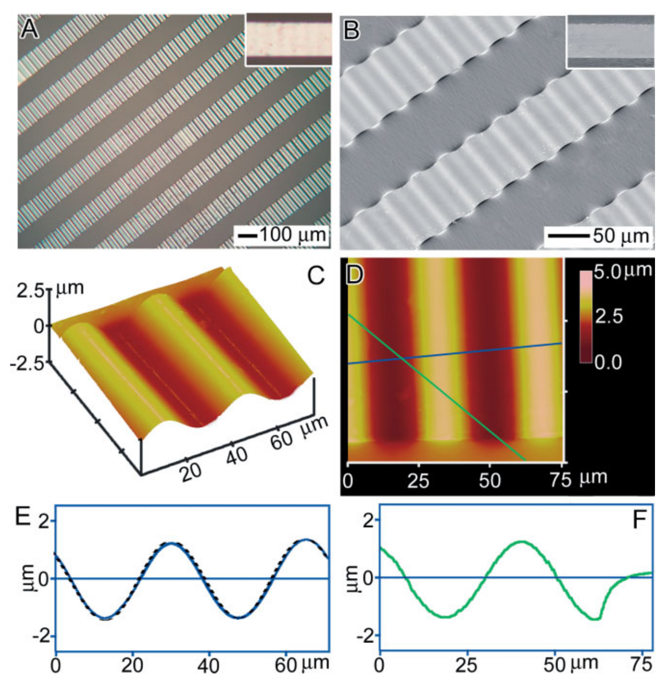

Figure 2. Images of wavy GaAs ribbons on a PDMS substrate, as formed with a prestrain of ca. 1.9 % generated through thermal expansion. A) Optical, B) scanning electron microscopy (SEM), C) 3D atomic force microscopy (AFM), and D) top view AFM images of the same sample. The SEM image was obtained by tilting the sample stage at an angle of 45° between sample surface and detection direction. (Spots on the ribbons might be residues from the sacrificial AlAs layers.) E,F) Surface height profiles plotted along the lines in blue and green as shown in (D), respectively.

the GaAs. A biaxial prestrain of ca. 1.9 % (calculated from the thermal response of PDMS)[28] was created in the PDMS by thermal expansion (heating to 90 °C in an oven) immediately prior to and during bonding. This heating also accelerated the formation of interfacial siloxane bonds. Cooling the PDMS to room temperature (ca. 27 °C) after transferring the GaAs ribbons released the prestrain. Frames A, B, and C of Figure 2 show optical microscopy, scanning electron microscopy (SEM), and atomic force microscopy (AFM) images, respectively, of the same sample. The images clearly show the formation of periodic, wavy structures in the GaAs ribbons. The waves were quantitatively analyzed by evaluating linecuts (Fig. 2E and F) from the AFM image in Figure 2D. The contour parallel to the longitudinal direction of the ribbon clearly shows a periodic, wavy profile, consistent with a computed fit to a sine wave (dashed line of Fig. 2E). This result agrees well with nonlinear analysis of the initial buckled geometry in a uniform, thin, high-modulus layer on a semi-infinite low-modulus support.[25,29] The peak-to-peak amplitude and wavelength associated with this function were determined to be 2.56 and 35.0 μm, respectively. The strains computed from the ratio of the horizontal distances between the adjacent two peaks on the stamp (i.e., the wavelength) to their actual contour lengths between the peaks (i.e., the surface distances measured by AFM), which we refer to as ribbon strains, yield values (ca. 1.3 %) that are smaller than the prestrain in the PDMS. This difference might be attributed to the low shear modulus of PDMS and island effects related to the length of GaAs ribbons being shorter than the length of the PDMS substrate.[30] The surface strains of GaAs ribbons at peaks and troughs, which we refer to as maximum GaAs strains, can be estimated from the ribbon thicknesses and radii of curvature at the peaks or troughs of the waves according to $\kappa h/2$, where κ is the curvature. In this evaluation, the direct contribution of strains in the PDMS stamp to the GaAs are ignored because the PDMS can be treated as a semi-infinite support whose modulus is low compared to that of GaAs (Young's modulus of GaAs = 85.5 GPa vs. that of PDMS = 2 MPa). For the data of Figure 2E, the maximum GaAs strains are ca. 0.62 %, which is more than a factor of two smaller than the ribbon strain (i.e., 1.3 %). This mechanical advantage provides stretchability in the GaAs ribbons, with physics similar to that in our recent report on wavy Si.

As shown in Figure 2F, the peak and trough regions of the ribbons are higher and lower than the contour level (right portion of the green curve) of the surface of pristine PDMS (i.e., the areas without ribbons), respectively. The result suggests that the PDMS under the GaAs adopts a wavy profile as a result of the upward and downward forces imparted to the PDMS by the GaAs ribbons in the peaks and troughs, respectively. The precise geometry of the PDMS near the peaks of the waves is very difficult to evaluate directly. We suspect that in addition to the upward deformation there is also a lateral necking caused by the Poisson effect. The wavy ribbons on the PDMS stamp can be stretched and compressed by applying strains to the PDMS (so-called *applied strain* denoted as positive for stretching and negative for compressing). The insets of Figure 2A and B show images of the ribbons stretched (ca. 1.5 %) to a flat geometry. Further stretching transfers more tensile strain to the flat GaAs ribbons, resulting in their breakage when this excess strain reaches the failure strain of GaAs. Compressive strains applied to the substrate reduce the wavelengths and increase the amplitudes of the wavy ribbons. Failure in compression occurs when the bending strains at peaks (and troughs) exceed the failure strains. This variation of wavelength with strain is consistent with previous observations in silicon, and is different from the predictions of wavelength invariance derived from ideal models.[29]

The stretchability of wavy GaAs ribbons can be improved by increasing the prestrain applied to PDMS through the use of a mechanical stage (as opposed to thermal expansion). For example, transferring GaAs ribbons with SiO_2 layers onto the surface of a PDMS stamp with prestrain of 7.8 % generated wavy ribbons without any observable cracking in the GaAs (Fig. 3A). In this case, the bending strains at the peaks are estimated to be ca. 1.2 %, which is lower than the failure strain (ca. 2 %) of GaAs. Similar to the low prestrain case, the wavy ribbons behave like an accordion when the system is stretched and compressed: the wavelengths and amplitudes change to accommodate the applied strain.[25] As shown in Figure 3A,

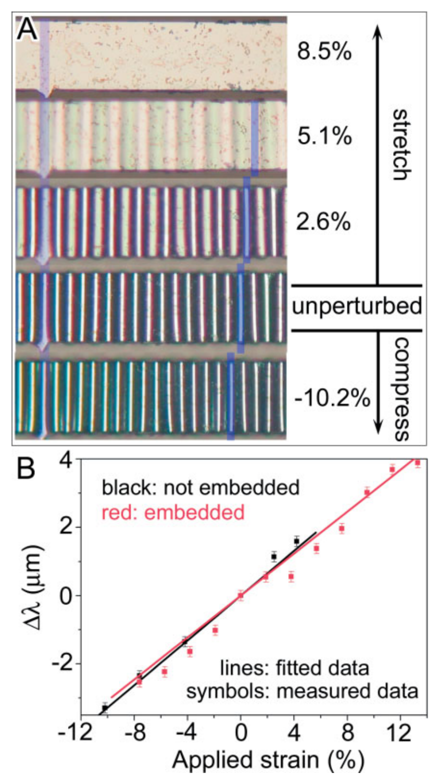

Figure 3. A) Optical microscopy images of wavy GaAs ribbons formed with a prestrain of 7.8 %, strongly bonded to the PDMS, collected at different applied strains. The blue bars on the left and right highlight certain peaks in the structure; the variation in the distance between these bars indicates the dependence of the wavelength on applied strain. B) Change in wavelength as a function of applied strain for the wavy GaAs ribbons shown in (A), plotted in black; similar data for a system of sample (A) after embedding in PDMS, plotted in red.

the wavelengths increase with tensile strain until the ribbons become flat and decrease with compressive strain until the ribbons break. These deformations are completely reversible, and do not involve any measurable slipping of the GaAs on the PDMS. The wavelength changes linearly with applied strains in both compression and tension (see, the black lines and symbols in Fig. 3B), in contrast to the mildly asymmetric behavior observed in Si ribbons with weak bonding and much lower prestrains.[25] The variation of wavelength with applied strains is in agreement with full finite element modeling of the mechanics of the system.

In practical applications, it might be useful to encapsulate the GaAs ribbons and devices in a way that maintains their stretchability. As a simple demonstration of one possibility, we cast and cured PDMS prepolymers on samples such as the one shown in Figure 3A to embed the ribbons in PDMS. The embedded systems exhibit similar mechanical behavior to the unembedded ones, i.e., stretching the system increases wavelength and compressing the system decreases wavelength (the red lines and symbols in Fig. 3B). Shrinkage resulting from curing of the second layer of PDMS generated some moderate amount of additional strain (ca. 1 %). This strain resulted in a slight decrease in the wavelength of the wavy ribbons, thereby expanding slightly the range of stretchability. Figure 3B shows the difference. Overall, the systems generated with prestrain of ca. 7.8 % can be stretched or compressed to strains of up to ca. 10 % without inducing any observable breakage in the GaAs.

The wavy GaAs ribbons on PDMS substrates can be used to fabricate high-performance electronic devices, such as MESFETs, the electrodes of which are formed through metallization and processing on the wafer, before transfer to PDMS. These metal layers change the flexural rigidity of the ribbons in a spatially dependent manner. Figure 4A shows GaAs ribbons integrated with ohmic stripes (source and drain electrodes) and Schottky contacts (gate electrodes) after transfer to a PDMS substrate with prestrain of ca. 1.9 %. The ohmic contacts consisted of metal stacks including AuGe (70 nm)/Ni (10 nm)/Au (70 nm) formed on the original wafers through lithographically defined masks along with sequential annealing of the wafers at elevated temperature (450 °C for 1 min) in a quartz tube with flowing N_2. These ohmic segments had lengths of 500 μm. The distances between two adjacent ohmic contacts were 500 μm (i.e., channel length). Schottky contacts with lengths of 240 μm (i.e., gate length) were generated by directly depositing a 75 nm Cr layer and a 75 nm Au layer through electron-beam evaporation against the photolithographically defined mask. The electrodes had widths equal to the GaAs ribbons, i.e., 100 μm; their relatively large sizes facilitate probing. (The dimensions of electrodes and semiconductor channels can be significantly decreased to achieve enhanced device performance.)[24] As shown in Figure 4A, these stretchable GaAs MESFETS exhibit, short-range, periodic waves only in the regions without electrodes. The absence of waves in the thicker regions might be attributed to their enhanced flexural rigidity mainly because of the additional thickness associated with the metals. Periodic waves could be initiated in the thicker regions by using prestrains larger than ca. 3 %. In these cases, however, the ribbons tend to break at the edges of the metal electrodes because of critical flaws and/or high peak strains near these edges. This failure mode limits the stretchability.

To circumvent this limitation, we reduced the strength of interaction between the MESFETs and the PDMS by eliminating the siloxane bonding. For such samples, prestrain > 3 % generated large, aperiodic buckles with relatively large widths and amplitudes because of physical detachment of the ribbons from the PDMS surface. Figure 4B presents this type of system, as prepared with a prestrain of ca. 7 %, in which the big buckles form in the thinner regions of the devices. The detachment seems to extend slightly to the thicker sections with ohmic stripes, as indicated by the vertical lines. The contrast variation along ribbons is attributed to reflections and refraction-associated passage of light through the curved GaAs segments. The SEM image (Fig. 4C) clearly shows the formation of arc-shaped buckles and flat, unperturbed PDMS. These buckles display asymmetric profiles (as indicated by the red

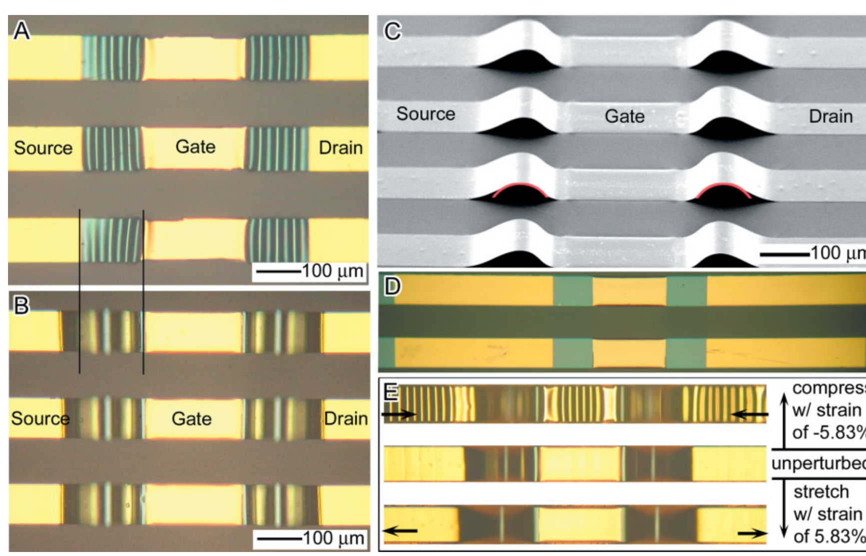

Figure 4. Images of GaAs ribbons integrated with ohmic (source and drain) and Schottky (gate) contacts to form complete MESFETs. A) Optical microscopy images of wavy ribbons formed using a prestrain of 1.9 % and strong bonding to the PDMS, showing the formation of periodic waves only in the sections without electrodes (grey). B) Optical and C) SEM images of buckled ribbons formed with a prestrain of ca. 7 % and weak bonding to the PDMS. D) Optical image of two buckled devices shown in (B) after they were stretched to be flat. E) A set of optical images of an individual ribbon device shown in (B) with different external applied strains (from top to bottom: compressing strain of 5.83 %, no applied strain, and stretching strain of 5.83 %) after it was embedded in PDMS.

curves) with tails with ohmic contacts to the sides. This asymmetry might be attributed to the unequal lengths (500 μm versus 240 μm) of ohmic stripes and Schottky contacts for individual transistors. This kind of buckled MESFET can be stretched to its original flat status (Fig. 4D) with applied stretching strains between ca. 6 % and ca. 7 %. However, compressing the system shown in Figure 4B leads to continuous detachment of ribbons from the PDMS surface to form larger buckles because of weak bonding. Embedding such devices in PDMS according to the previously described procedures eliminates this type of uncontrolled behavior. Figure 4B shows such a system, in which the liquid PDMS precursor fills the gaps underneath the buckles. The fully surrounding PDMS confines the ribbons and prevents them from sliding and detaching. The embedded devices can be reversibly stretched and compressed to strains up to ca. 6 % without breaking the ribbons. It is notable that when the embedded system was compressed by –5.83 % (top frame of Fig. 4E), periodic, small waves formed in the regions with metal electrodes as well as new ripples in the buckled regions. The formation of these new small waves in combination with the large buckles enhances the compressibility. Stretching the system forces the buckled regions to compress and stretch the PDMS in a manner that enables some flattening of these buckles, thereby elongating the projected lengths of the ribbons (bottom frame of Fig. 4E). These results suggest that embedded devices with big buckles, which are a kind of geometry distinct from the waves, represent a promising method to achieve stretchability and compressibility that can be used in combination with or separately from the wavy approach.

The performance of buckled devices can be evaluated by directly probing the current flow from source to drain. Figure 5A shows GaAs-ribbon devices fabricated on a wafer, picked up using a flat PDMS stamp and transfer printed onto a PDMS substrate with a prestrain of 4.7 %. In this configuration, the metal electrodes are exposed to air for electrical probing. After the prestretched PDMS was relaxed to a strain of 3.4 %, periodic small waves formed in the thin regions of the MESFET (the second frame of Fig. 5A). When the prestretched PDMS stamp was fully relaxed, the small waves in each segment of pure GaAs coalesced into an individual big buckle (the third frame of Fig. 5A). The buckled devices could be stretched to their flat status with an applied stretching strain of 4.7 % (see the bottom frame of Figure 5A). The current–voltage (*I–V*) curves of the same device with applied strains of 0.0 % (the third frame of Fig. 5A) and 4.7 % (the bottom frame of Fig. 5A) are plotted in Figure 5B with red and black colors, respectively. The results indicate that the current flow from source to drain of buckled MESFETs on PDMS substrates can be well modulated with the voltages applied to the gate and that the applied stretching strain generates only a minor effect on device performance.

In summary, an approach has been developed to form "buckled" and "wavy" GaAs ribbons onto or embedded in PDMS elastomeric substrates. The geometrical configurations of these ribbons depend on the levels of prestrains used in the fabrication, the strength of interactions between the PDMS and ribbons, and on the thicknesses and types of materials used. Buckled and wavy ribbons of GaAs multilayer stacks and fully formed MESFET devices show large levels of compressibility/stretchability, because of the ability of their geometries to adjust in a manner that can accommodate applied strains without transferring those strains to the materials themselves. Successful realization of large levels of mechanical stretchability (and, as a result, other attractive mechanical characteristics such as extreme bendability) in an intrinsically fragile material like GaAs suggests that similar strategies might be applicable to a wide range of other materials classes. These possibilities, alternative geometrical strategies to achieve similar mechanical characteristics, and detailed mechanical modeling of these systems represent topics of current work.

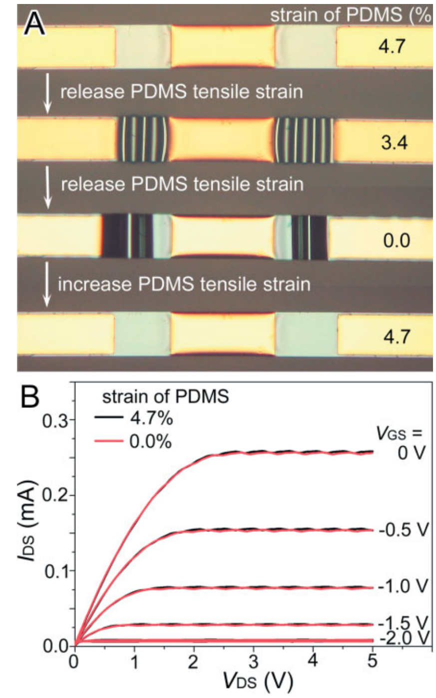

Figure 5. A) Optical images of a GaAs ribbon MESFET on a PDMS stamp with different strains built into the PDMS substrate. The prestrain applied to the PDMS stamp was 4.7 % before the devices were transferred onto its surface. B) Comparison of drain source current–voltage (*I–V*) curves for the device shown in (A) before and after 4.7 % stretching strain was applied to the system; I_{DS}: drain-source current, V_{DS}: drain-source voltage.

Experimental

GaAs wafers with custom-designed epitaxial layers (details described in the text) were purchased from IQE Inc., Bethlehem, PA. The lithographic processes employed AZ photoresist, i.e., AZ 5214 and AZ nLOF 2020 for positive and negative imaging, respectively. The GaAs wafers with photoresist mask patterns were anisotropically etched in the etchant (4 mL H_3PO_4 (85 wt %), 52 mL H_2O_2 (30 wt %), and 48 mL deionized water) that was cooled in the ice–water bath. The AlAs layers were dissolved with a diluted HF solution (Fisher Chemicals) in ethanol (1:2 in volume). The samples with released ribbons on mother wafers were dried in a fume hood. The dried samples were placed in the chamber of an electron-beam evaporator (Temescal FC-1800) and were coated with sequential layers of 2 nm Ti and 28 nm SiO_2. The metals for the MESFET devices were deposited by electron-beam evaporation before removal of the AlAs layers. A PDMS stamp with thickness of ca. 5 mm was prepared by pouring the mixture of low-modulus PDMS (component ratio A:B = 1:10, Sylgard 184, Dow Corning) onto a piece of silicon wafer premodified with monolayer of (tridecafluoro-1,1,2,2-tetrahydrooctyl)-1-trichlorosilane, followed by baking at 65 °C for 4 h. In order to generate strong bonding, the stamps were exposed to UV light in air for 5 min. In the transfer process, the stamps were stretched through thermal expansion (in oven) and/or mechanical forces. The wafers with released ribbons were then laminated on the surfaces of the stretched PDMS stamps and left in contact at elevated temperatures (dependent on the required prestrains) for 5 min. The mother wafers were peeled from the stamps and all the ribbons were transferred to stamps. The prestrains applied to the stamps were released through cooling down to room temperature and/or removing the mechanical forces, resulting in the formation of wavy profiles along ribbons. In the mechanical evaluations, we used a specially designed stage to stretch as well as compress the PDMS stamps with “wavy” and “buckled” GaAs ribbons.

Received: March 26, 2006
Published online: October 10, 2006

[1] R. H. Reuss, B. R. Chalamala, A. Moussessian, M. G. Kane, A. Kumar, D. C. Zhang, J. A. Rogers, M. Hatalis, D. Temple, G. Moddel, B. J. Eliasson, M. J. Estes, J. Kunze, E. S. Handy, E. S. Harmon, D. B. Salzman, J. M. Woodall, M. A. Alam, J. Y. Murthy, S. C. Jacobsen, M. Olivier, D. Markus, P. M. Campbell, E. Snow, *Proc. IEEE* **2005**, *93*, 1239.

[2] K. Jain, M. Klosner, M. Zemel, S. Raghunandan, *Proc. IEEE* **2005**, *93*, 1500.

[3] A. Nathan, B.-K. Park, Q. Ma, A. Sazonov, J. A. Rowlands, *Microelectron. Reliab.* **2002**, *42*, 735.

[4] a) H. Sirringhaus, *Adv. Mater.* **2005**, *17*, 2411. b) S. R. Forrest, *Nature* **2004**, *428*, 911. c) C. R. Newman, C. D. Frisbie, D. A. da Silva, J.-L. Brédas, P. C. Ewbank, K. R. Mann, *Chem. Mater.* **2004**, *16*, 4436. d) H. E. Katz, Z. Bao, S. Gilat, *Acc. Chem. Res.* **2001**, *34*, 359. e) H. E. Katz, *Chem. Mater.* **2004**, *16*, 4748. f) Y. Sun, Y. Liu, D. Zhu, *J. Mater. Chem.* **2005**, *15*, 53.

[5] a) D. Knipp, R. A. Street, A. Völkel, J. Ho, *J. Appl. Phys.* **2003**, *93*, 347. b) C.-W. Chu, S.-H. Li, C.-W. Chen, V. Shrotriya, Y. Yang, *Appl. Phys. Lett.* **2005**, *87*, 193 508. c) B. S. Ong, Y. Wu, P. Liu, *Proc. IEEE* **2005**, *93*, 1412.

[6] a) G. H. Gelinck, H. E. A. Juitema, E. Van Veenendaal, E. Cantatore, L. Schrijnemakers, J. B. P. H. Van der Putten, T. C. T. Geuns, M. Beenhakkers, J. B. Giesbers, B.-H. Huisman, E. J. Meijer, E. M. Benito, F. J. Touwslager, A. W. Marsman, B. J. E. Van Rens, D. M. de Leeuw, *Nat. Mater.* **2004**, *3*, 106. b) J. A. Rogers, Z. Bao, K. Baldwin, A. Dodabalapur, B. Crone, V. R. Raju, V. Kuck, H. Katz, K. Amundson, J. Ewing, P. Drzaic, *Proc. Natl. Acad. Sci. USA* **2001**, *98*, 4935. c) T. Someya, Y. Kato, S. Iba, Y. Noguchi, T. Sekitani, H. Kawaguchi, T. Sakurai, *IEEE Trans. Electron Devices* **2005**, *52*, 2502. d) T. Someya, Y. Kato, T. Sekitani, S. Iba, Y. Noguchi, Y. Murase, H. Kawaguchi, T. Sakurai, *Proc. Natl. Acad. Sci. USA* **2005**, *102*, 12 321.

[7] a) V. C. Sundar, J. Zaumseil, V. Podzorov, E. Menard, R. L. Willett, T. Someya, M. E. Gershenson, J. A. Rogers, *Science* **2004**, *303*, 1644. b) E. Menard, V. Podzorov, S.-H. Hur, A. Gaur, M. E. Gershenson, J. A. Rogers, *Adv. Mater.* **2004**, *16*, 2097. c) V. Podzorov, E. Menard, J. A. Rogers, M. E. Gershenson, *Phys. Rev. Lett.* **2005**, *95*, 226 601. d) W.-Y. Chou, H.-L. Cheng, *Adv. Funct. Mater.* **2004**, *14*, 811. e) M. Mas-Torrent, P. Hadley, N. Crivillers, J. Veciana, C. Rovira, *ChemPhysChem* **2006**, *7*, 86.

[8] a) M. Halik, H. Klauk, U. Zschieschang, G. Schmid, C. Dehm, M. Schütz, S. Maisch, F. Effenberger, M. Brunnbauer, F. Stellacci, *Nature* **2004**, *431*, 963. b) M.-H. Yoon, H. Yan, A. Facchetti, T. J. Marks, *J. Am. Chem. Soc.* **2005**, *127*, 10 388. c) Y. Jang, D. H. Kim, Y. D. Park, J. H. Cho, M. Hwang, K. Cho, *Appl. Phys. Lett.* **2006**, *88*, 072 101.

[9] a) M. C. Hamilton, S. Martin, J. Kanicki, *Chem. Mater.* **2004**, *16*, 4699. b) M. J. Deen, M. H. Kazemeini, Y. M. Haddara, J. Yu, G. Vamvounis, S. Holdcroft, W. Woods, *IEEE Trans. Electron Devices* **2004**, *51*, 1892. c) K. Cheng, M.-H. Yang, W. W. W. Chiu, C.-Y. Huang, J. Chang, T.-F. Ying, Y. Yang, *Macromol. Rapid Commun.* **2005**, *26*, 247.

[10] a) E. Fortunato, L. Pereira, H. Águas, I. Ferreira, R. Martins, *Proc. IEEE* **2005**, *93*, 1281. b) A. Sazonov, D. Striakhilev, C.-H. Lee, A. Nathan, *Proc. IEEE* **2005**, *93*, 1420. c) A. J. Flewitt, W. I. Milne, *Proc. IEEE* **2005**, *93*, 1364. d) P. Servati, A. Nathan, *Proc. IEEE* **2005**, *93*, 1257.

[11] a) C.-S. Yang, L. L. Smith, C. B. Arthur, G. N. Parsons, *J. Vac. Sci. Technol. B* **2000**, *18*, 683. b) P. I. Hsu, H. Gleskova, M. Huang, Z. Suo, S. Wagner, J. C. Sturm, *J. Non-Cryst. Solids* **2002**, *299–302*, 1355.

[12] Y. Chen, J. Au, P. Kazlas, A. Ritenour, H. Gates, M. McCreary, *Nature* **2003**, *423*, 136.

[13] a) M. Wu, S. Wagner, *Appl. Phys. Lett.* **2001**, *78*, 3729. b) S. Wagner, H. Gleskova, I.-C. Cheng, M. Wu, *Thin Solid Films* **2003**, *430*, 15. c) M. Wu, S. Wagner, *Appl. Surf. Sci.* **2001**, *175–176*, 753.

[14] a) S. V. Karnik, M. K. Hatalis, *Jpn. J. Appl. Phys., Part 1* **2003**, *42*, 1200. b) S. V. Karnik, M. K. Hatalis, *Solid-State Electron.* **2003**, *47*, 653.

[15] P. K. Shetty, N. D. Theodore, J. Ren, J. Menendez, H. C. Kim, E. Misra, J. W. Mayer, T. L. Alford, *Mater. Lett.* **2005**, *59*, 872.

[16] A. Imparato, C. Minarini, A. Rubino, P. Tassini, F. Villani, D. D. Sala, E. Amendola, M. Kunst, H.-C. Neitzert, S. Bellone, *Thin Solid Films* **2005**, *487*, 58.

[17] X. Duan, C. Niu, V. Sahi, J. Chen, J. W. Parce, S. Empedocles, J. L. Goldman, *Nature* **2003**, *425*, 274.

[18] M. C. McAlpine, R. S. Friedman, S. Jin, K.-H. Liu, W. U. Wang, C. M. Lieber, *Nano Lett.* **2003**, *3*, 1531.

[19] E. Menard, K. J. Lee, D.-Y. Khang, R. G. Nuzzo, J. A. Rogers, *Appl. Phys. Lett.* **2004**, *84*, 5398.

[20] E. Menard, R. G. Nuzzo, J. A. Rogers, *Appl. Phys. Lett.* **2005**, *86*, 093 507.

[21] Z.-T. Zhu, E. Menard, K. Hurley, R. G. Nuzzo, J. A. Rogers, *Appl. Phys. Lett.* **2005**, *86*, 133 507.

[22] K. J. Lee, M. J. Motala, M. A. Meitl, W. R. Childs, E. Menard, A. K. Shim, J. A. Rogers, R. G. Nuzzo, *Adv. Mater.* **2005**, *17*, 2332.

[23] Y. Sun, S. Kim, I. Adesida, J. A. Rogers, *Appl. Phys. Lett.* **2005**, *87*, 083 501.

[24] Y. Sun, E. Menard, J. A. Rogers, H.-S. Kim, S. Kim, G. Chen, I. Adesida, R. Dettmer, R. Cortez, A. Tewksbury, *Appl. Phys. Lett.* **2006**, *88*, 183 509.

[25] D.-Y. Khang, H. Jiang, Y. Huang, J. A. Rogers, *Science* **2006**, *311*, 208.

[26] Y. Sun, J. A. Rogers, *Nano Lett.* **2004**, *4*, 1953.

[27] Y. Sun, D.-Y. Khang, F. Hua, K. Hurley, R. G. Nuzzo, J. A. Rogers, *Adv. Funct. Mater.* **2005**, *15*, 30.

[28] The thermally induced prestrain is ascribed to thermal expansion of the PDMS stamp, which has a bulk linear coefficient of thermal expansion of $\alpha_L = 3.1 \times 10^{-4}\ \mu m\,\mu m^{-1}\,°C^{-1}$. T. Buma, M. Spisar, M. O'Donnell, *Appl. Phys. Lett.* **2001**, *79*, 548. On the other hand, the coefficient of thermal expansion for GaAs is only $5.73 \times 10^{-6}\ \mu m\,\mu m^{-1}\,°C^{-1}$. Therefore, the prestrain on PDMS (relatively GaAs ribbons) for the sample that was prepared at 90 °C and cooled down to 27 °C was determined according to $\Delta\alpha_L \cdot \Delta T = (3.1 \times 10^{-4} - 5.73 \times 10^{-6}) \times (90 - 27) = 1.9\,\%$.

[29] Z. Y. Huang, W. Hong, Z. Suo, *J. Mech. Phys. Solids* **2005**, *53*, 2101.

[30] S. Wagner, S. P. Lacour, J. Jone, P.-H. I. Hsu, J. C. Sturm, T. Li, Z. Suo, *Phys. E* **2005**, *25*, 326.

